

# UV Irradiation to Increase the Spectral Sensitivity of a-SiC:H pi'n/pin Photodiode Beyond the Visible Spectrum Light

M. Vieira, M.A. Vieira, V. Silva, P. Louro, A. Fantoni  
 CTS/UNINOVA  
 Monte de Caparica, Portugal  
 e-mail: mv@isel.ipl.pt

M. Vieira, M.A. Vieira, I. Rodrigues, V. Silva, P.  
 Louro, A. Fantoni  
 DEETC/ISEL  
 Lisbon, Portugal  
 e-mail: mv@isel.ipl.pt

**Abstract**— In this paper, we experimentally demonstrate the use of near-ultraviolet steady state illumination to increase the spectral sensitivity of a double a-SiC/Si pi'n/pin photodiode beyond the visible spectrum (400 nm-880 nm). The concept is extended to implement a 1 by 4 wavelength division multiplexer with channel separation in the visible/near infrared ranges. The device consists of a p-i'(a-SiC:H)-n/p-i(a-Si:H)-n heterostructure, sandwiched between two transparent contacts. Optoelectronic characterization of the device is presented and shows the feasibility of tailoring the wavelength and bandwidth of a polychromatic mixture of different wavelengths. Results show that the spectral current under steady state ultraviolet irradiation depends strongly on the wavelength of the impinging light, and on the background intensity and irradiation side allowing controlled high-pass filtering properties. If several monochromatic pulsed lights, in the visible/ Near infrared (VIS/NIR) range, separately or in a polychromatic mixture illuminate the device, data shows that, front background enhances the light-to-dark sensitivity of the medium, long and infrared wavelength channels, and quench strongly the low wavelengths channels. Back background has the opposite behavior; it enhances only channel magnitude in short wavelength range and strongly reduces it in the long ones. This nonlinearity provides the possibility for selective tuning of a specific wavelength. A capacitive optoelectronic model supports the experimental results. A numerical simulation is presented.

**Keywords**- *amorphous SiC technology; optoelectronics; spectral sensitivity; UV irradiation; photodiode; multiplexer device; VIS/NIR decoding; numerical simulation.*

## I. INTRODUCTION

The LED is a very effective lighting technology due to its high brightness, long life, energy efficiency, durability, affordable cost, optical spectrum and its colour range for creative purposes. Their application as communication device with a photodiode as receptor, has been used for many years in hand held devices, to control televisions and other media equipment, and with higher rates between computational devices [1]. This communication path has been employed in the near infra-red (NIR) range, but due to the increasing LED lighting in homes and offices, the idea to

use them for visible light communications (VLC) has come up recently. Newly developed technologies, for infrared telecommunication systems, allow increase of capacity, distance, and functionality, leading to the design of new reconfigurable active filter [2], [3], [4]. To enhance the transmission capacity and the application flexibility of optical communication, efforts have to be considered, namely the fundamentals of Wavelength Division Multiplexer (WDM) based on a-SiC:H light controlled filters, when different visible signals are encoded in the same optical transmission path [5]. They can be used to achieve different filtering processes, such as: amplification, switching, and wavelength conversion.

In this paper, it is demonstrated that the same a-SiC:H device under front and back controlled near ultraviolet optical bias acts as a reconfigurable active filter in the visible and near infrared ranges, making the bridge between the infrared and the red spectral ranges. In consequence, bridging the visible spectrum to the telecom gap offers the opportunity to provide alternative and additional low cost services to improve operative production processes in office, home and automotive networks.

In Section I, an introduction is given and in Section II, some experimental results are presented. In Section III, the bias controlled selector is analyzed and in Section IV, the Wavelength Division Multiplexed (WDM) based on SiC technology is described. In Section V, the optoelectronic model gives insight the physics of the device and finally in Section VI, the conclusions are presented.

## II. EXPERIMENTAL DETAILS

### A. Device configuration

The light tunable filter is realized by using a double pi'n/pin a-SiC:H photodetector produced by Plasma Enhanced Chemical Vapor Deposition (PECVD).

The device has Transparent Conductive Oxide (TCO) front and back biased optical gating elements as depicted in Figure 1.

The active device consists of a p-i'(a-SiC:H)-n/p-i(a-Si:H)-n heterostructure with low conductivity doped layers. The deposition conditions and optoelectronic characterization of the single layers were described elsewhere [6].

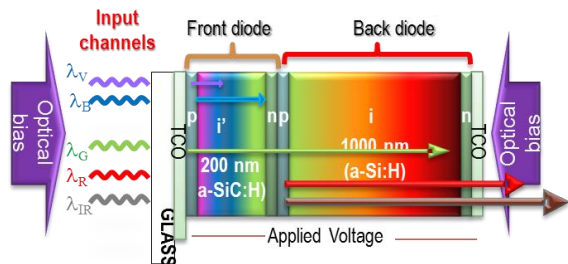


Figure 1. Device configuration and operation.

The thicknesses and optical gap of the front i' (200 nm; 2.1 eV) and back i (1000 nm; 1.8 eV) layers are optimized for light absorption in the blue and red ranges, respectively [7].

B. Device operation

Monochromatic (infrared, red, green, blue and violet;  $\lambda_{IR,R,G,B,V}$ ) pulsed communication channels (input channels) are combined together, each one with a specific bit sequence, impinge on the device and are absorbed accordingly to their wavelengths (see arrow magnitudes in Figure 1).

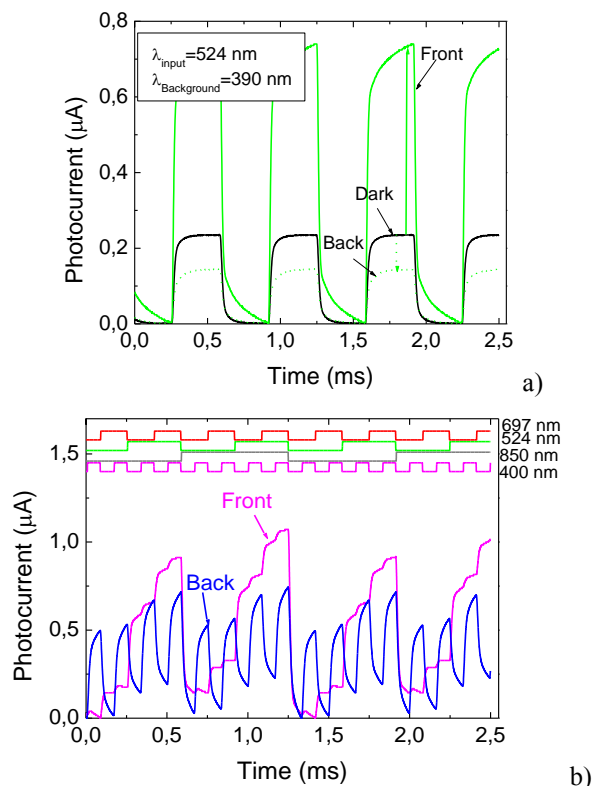


Figure 2. a) 524 nm input channel under front, back and without (dark) background irradiation. b) MUX signals and under front and back  $\lambda=390$  nm irradiation and different bit sequences.

The combined optical signal (multiplexed signal; MUX) is analyzed by reading out the generated photocurrent under negative applied voltage (-8V), without and with near ultraviolet background ( $\lambda_{Background}=390$  nm) and different intensities, applied either from the front ( $\lambda_F$ ) or the back ( $\lambda_B$ ) sides. The device operates within the visible range using as input color channels the square wave modulated low power light supplied by near-infrared/visible (VIS/NIR) LEDs. In Figure 2a, the 524 nm input channel is displayed under front, back and without UV irradiation. The arrows indicate the enhancement (solid line) or quenching (dot line) of the dark signal, respectively under front and back irradiation. In Figure 2b, the polychromatic mixture of four different input channels (400 nm, 524 nm, 697nm and 850 nm) under front and back  $2800 \mu Wcm^{-2}$  irradiation, is displayed. At the top, the input channels wavelengths and their bit sequences guide the eyes.

III. BIAS CONTROLLED SELECTOR

A. Optical bias controlled filter

The spectral sensitivity was tested through spectral response measurements [8] without and under 390 nm front and back backgrounds of variable intensities. The spectral gain ( $\alpha$ ), defined as the ratio between the signal with and without irradiation was inferred.

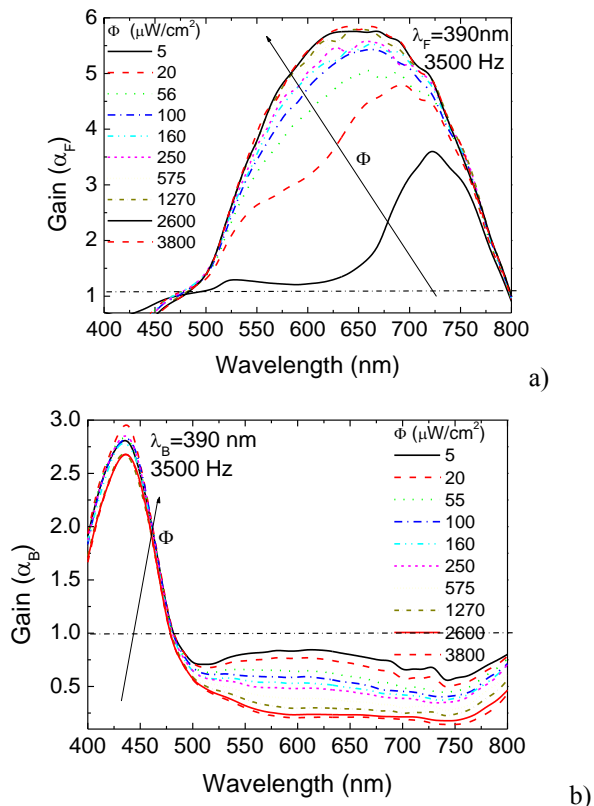


Figure 3. Front ( $\lambda_F$ ) and back ( $\lambda_B$ ) spectral gains ( $\alpha_{F,B}$ ) respectively, under  $\lambda=390$  nm irradiations.

In Figure 3, the spectral gain ( $\alpha$ ) is displayed under steady state irradiations. In Figure 3a, the light was applied from the front ( $\lambda_F$ ) and in Figure 3b, the irradiation occurs from the back side ( $\lambda_B$ ). The background intensity ( $\phi$ ) was changed between  $5 \mu\text{Wcm}^{-2}$  and  $3800 \mu\text{Wcm}^{-2}$ .

Results show that, the optical gains have opposite behaviors. Under front irradiation (Figure 3a) and low flux, the gain is high in the infrared region, presents a well-defined peak at 725 nm and strongly quenches in the visible range. As the power intensity increases, the peak shifts to the visible range and can be deconvoluted into two peaks, one in the red range that slightly increases with the power intensity of the background and another in the green range that strongly increases with the intensity of the ultraviolet (UV) radiation. In the blue range, the gain is much lower. This shows the controlled high-pass filtering properties of the device under different background intensities. Under back bias (Figure 3b) the gain in the blue/violet range has a maximum near 420 nm that quickly increases with the intensity. Moreover, it strongly lowers for wavelengths higher than 450 nm, acting as a short-pass filter. Thus, back irradiation, tunes the violet/blue region of the visible spectrum whatever the flux intensity, while front irradiation, depending on the background intensity, selects the infrared or the visible spectral ranges. Here, low fluxes select the near infrared region and cuts the visible one, the reddish part of the spectrum is selected at medium fluxes, and high fluxes tune the red/green ranges with different gains.

**B. Nonlinear spectral gain**

To analyze the effect of the background intensity in the input channels, several monochromatic pulsed lights separately (850 nm, 697 nm, 626 nm, 524 nm, 470 nm, 400 nm; input channels) or combined (MUX signal) illuminated the device at 12000 bps [9].

Steady state optical bias with different intensities was superimposed separately from the front and back sides and the photocurrent measured. For each individual channel the photocurrent gain under irradiation was determined. In Figure 4, these gains are displayed as a function of the background lighting under front (Figure 4a) and back (Figure 4b) irradiation.

Results show that, even under transient conditions and using commercial visible and NIR LEDs, the background side and intensity alters the signal magnitude of the input channels.

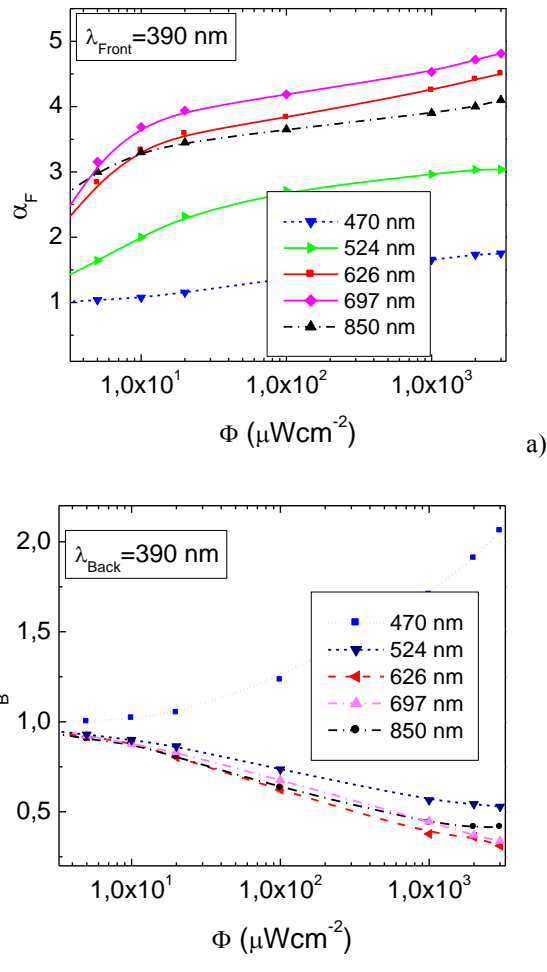


Figure 4. Front (a) and back (b) optical gains as a function of the background intensity for different input wavelengths in the VIS/NIR range.

The gain depends mainly on the channel wavelength and to some extent on the lighting intensity. Even across narrow bandwidths, the photocurrent gains are quite different. This nonlinearity allows identification of the different input channels in the visible/infrared ranges.

**IV. WAVELENGTH DIVISION MULTIPLEXER**

**A. Input channels**

Four monochromatic pulsed lights with different intensities, separately (400 nm, 470 nm, 697 nm and 850 nm; input channels) or combined (MUX signal) illuminated the device at 12000 bps.

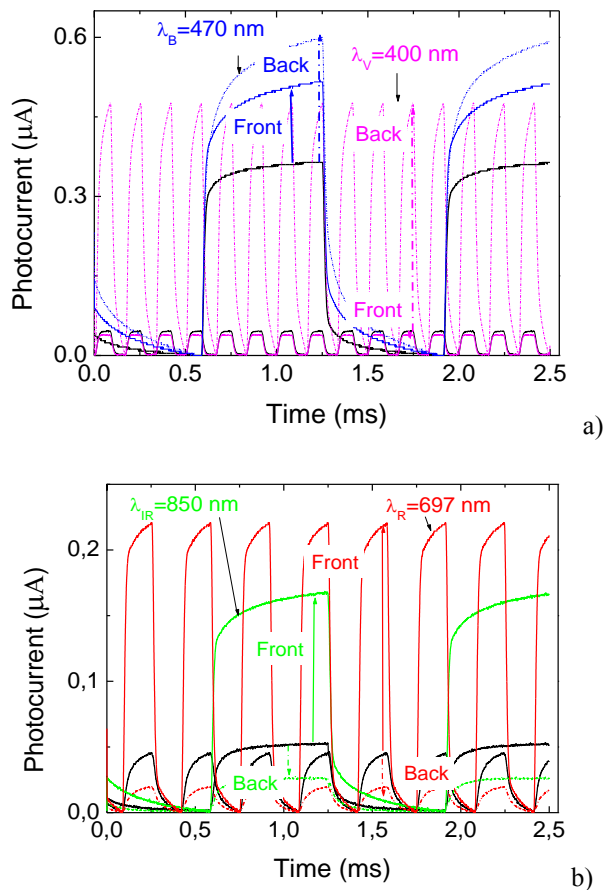


Figure 5. Input signals under front and back 390 nm background irradiation. a) violet and blue channels. b) red and infrared channels.

Steady state 390 nm front and back optical bias with  $2800 \mu\text{Wcm}^{-2}$  intensity was superimposed separately and the photocurrent was measured. In Figure 5a, the blue and violet transient signals are presented under front and back irradiations while in Figure 5b, the red and infrared signals are displayed.

In Table I, the measured optical gains for five different input channels are displayed.

TABLE I OPTICAL GAINS UNDER 390 NM FRONT ( $\alpha_{\text{FRONT}}$ ) AND BACK ( $\alpha_{\text{BACK}}$ ) IRRADIATIONS.

	$\lambda=400$ nm	$\lambda=470$ nm	$\lambda=524$ nm	$\lambda=697$ nm	$\lambda=850$ nm
$\alpha_{\text{Back}}$	11.6	1.8	0.61	0.46	0.44
$\alpha_{\text{Front}}$	0.9	1.5	3.2	4.3	3.5

Back irradiation enhances, differently, the input signals in the short wavelength range (Figure 5a) while front irradiation increases them otherwise in the long wavelength range (Figure 5b). This side dependent effect is used to enhance or to quench the input signals allowing their recognition and providing the possibility for selective tuning of the visible and IR input channels.

B. MUX signal

In Figure 6, two MUX signals due to the input signals of Figure 2a and Figure 5 are displayed without (dark) and under front and back irradiation. On top, the signals used to drive the input channels are shown to guide the eyes into the on/off channel states.

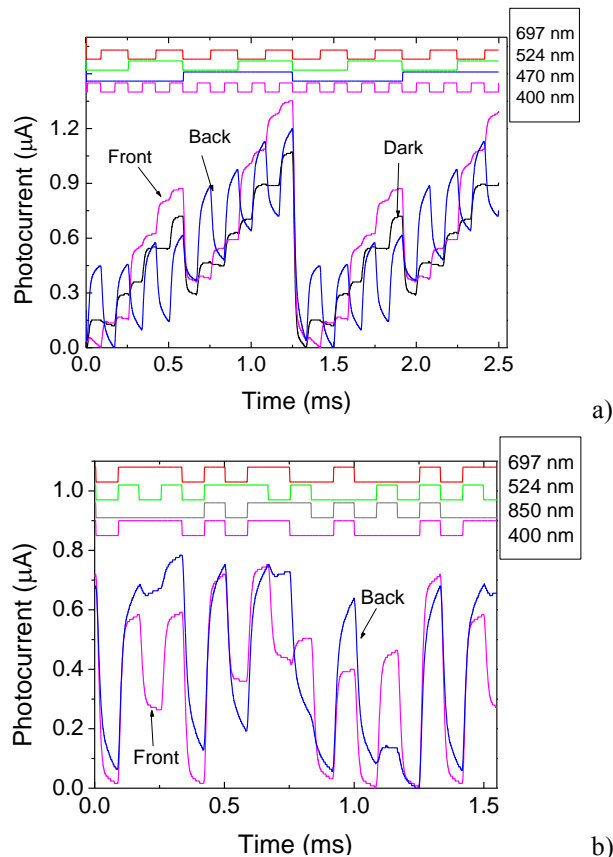


Figure 6. MUX signals: a) without and under front and back  $\lambda=390$  nm irradiation and different bit sequences. b) Front and back irradiation and two channels (400 nm and 697 nm) with the same bit sequence.

Results show that, the background side alters the form of the MUX signal, enhancing or quenching different spectral ranges. In Figure 6a all the on/off states are possible so, without optical bias,  $2^4$  ordered levels are detected and correspond to all the possible combinations of the on/off states. Under, either front or back irradiation, each of those four channels, by turn, are enhanced or quenched differently (Figure 6, Table I) resulting in an increase magnitude of red/green under front irradiation or of the blue/violet one, under back lighting. Since the gain of the four input channels is different ( $\alpha_{F,B}$ ; Table I) this nonlinearity allows identifying the different input channels in a large visible/infrared range. In Figure 6b, both 400 nm and 697 nm channels have the same bit sequence which corresponds to only  $2^3$  ordered levels, however once the optical gains of both channels are quite different under front and back irradiation (Table I) it is possible to identify them. Under back irradiation the MUX

signal receive its main contribution from the 400 nm channel while under front irradiation it is mainly weighed buy the long wavelength channels. By comparing front and back irradiation is possible to decode the transmitted information.

Under front irradiation, near-UV radiation is absorbed at the beginning of the front diode and, due to the self-bias effect, increases the electric field at the back diode where the red/infrared incoming photons (see Figure 1) are absorbed accordingly to their wavelengths (see Figure 3) resulting in an increased collection. Under back irradiation the electric field decreases mainly at the back i-n interface enhancing the electric field at the front diode quenching it at the back one. This leads to an increased collection of the violet/blue input signals.

So, by switching between front to back irradiation the photonic function is modified from a long- to a short-pass filter allowing, alternately selecting the red/infrared channels or the blue and violet ones, thus, making the bridge between the visible and the infrared regions.

V. OPTOELECTRONIC MODEL

Based on the experimental results and device configuration a two connected phototransistors model (Figure 7a), made out of a short- and a long-pass filter was developed [5] and upgraded to include several input channels. The *ac* circuit representation is displayed in Figure 7b and is supported by the complete dynamical large signal Ebers-Moll model with series resistances and capacities. The charge stored in the space-charge layers is modelled by the capacitor  $C_1$  and  $C_2$ .  $R_1$  and  $R_2$  model the dynamical resistances of the internal and back junctions under different *dc* bias conditions. The operation is based upon the following strategic principle: the flow of current through the resistor connecting the two transistor bases is proportional to the difference in the voltages across both capacitors (charge storage buckets). The modified electrical model developed is the key of this strategic operation principle. Two optical gate connections ascribed to the different light penetration depths across the front ( $Q_1$ ) and back ( $Q_2$ ) phototransistors were considered to allow independent blue ( $I_1$ ), red/infrared ( $I_2$ ) and green ( $I_3, I_4$ ) channels transmission. Four square-wave current sources with different intensities are used; two of them,  $I_1$  and  $I_2$ , with different frequencies to simulate the input blue and red channels and the other two,  $I_3$  and  $I_4$ , with the same frequency but different intensities, to simulate the green channel due to its asymmetrical absorption across both front and back phototransistors.

In Figure 7c, the block diagram of the optoelectronic state model is displayed. The resistors ( $R_1, R_2$ ) and capacitors ( $C_1, C_2$ ) synthesize the desired filter characteristics. The input signals,  $\lambda_{IR,R,G,B,V}$  model the input channels and  $i(t)$  the output signal. The amplifying elements,  $\alpha_1$  and  $\alpha_2$  are linear combinations of the optical gains of each impinging channel, respectively into the front and back phototransistors and account for the enhancement or quenching of the channels (Figure 3) due to the steady state irradiation. Under front irradiation we have:  $\alpha_2 \gg \alpha_1$  and under back irradiation  $\alpha_1 \gg \alpha_2$ . This affects the reverse photo

capacitances,  $(\alpha_{1,2}/C_{1,2})$  that determine the influence of the system input on the state change.

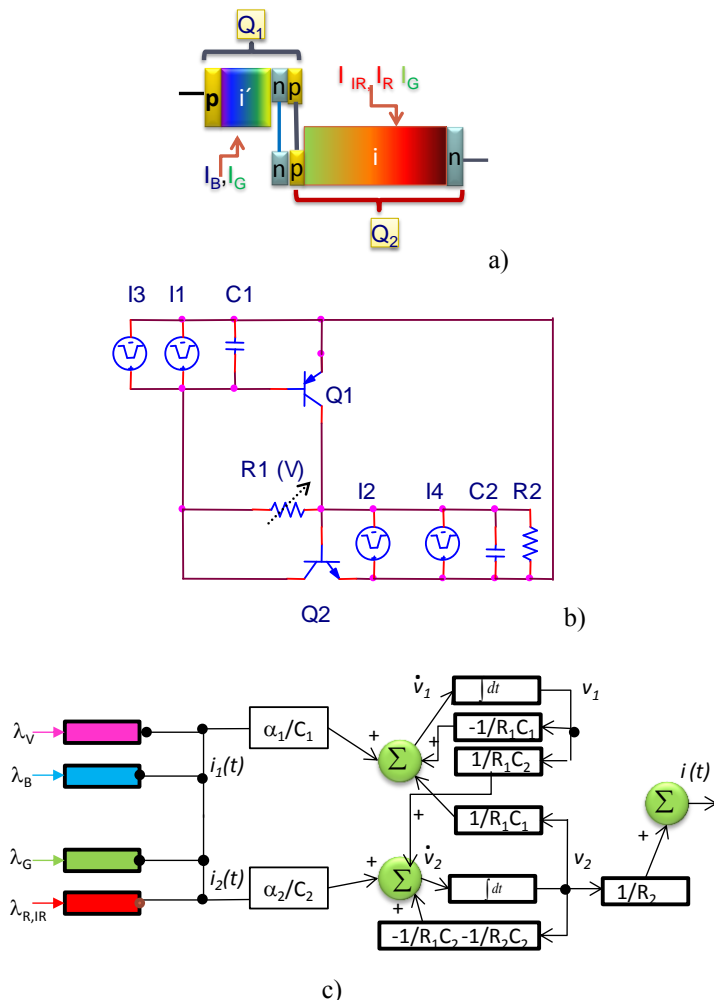


Figure 7. a) Two connected transistor model, b) equivalent electric circuit, c) block diagram of the optoelectronic state model.

A graphics user interface computer program was designed and programmed within the MATLAB® programming language, to ease the task of numerical simulation. This interface allows selecting model parameters, along with the plotting of bit signals and both simulated and experimental photocurrent results. To simulate the input channels we have used the individual magnitude of each input channel without background lighting (Figures 2 and 5), and the corresponding gain at the simulated background intensity (Table I). Figure 8, presents results of a numerical simulation with  $3000 \mu\text{W}/\text{cm}^2$  front and back  $\lambda=390 \text{ nm}$  irradiation and the experimental outputs of Figure 2b and Figure 6b, respectively.

Values of  $R_1=10 \text{ K}\Omega$ ,  $R_2=1 \text{ K}\Omega$ ,  $C_1=1000 \text{ pF}$ ,  $C_2=20000 \text{ pF}$  were used during the simulation process (Figure 7c). On top of the figures, the drive input LED signals guide the eyes into the different *on/off* states and correspondent wavelengths

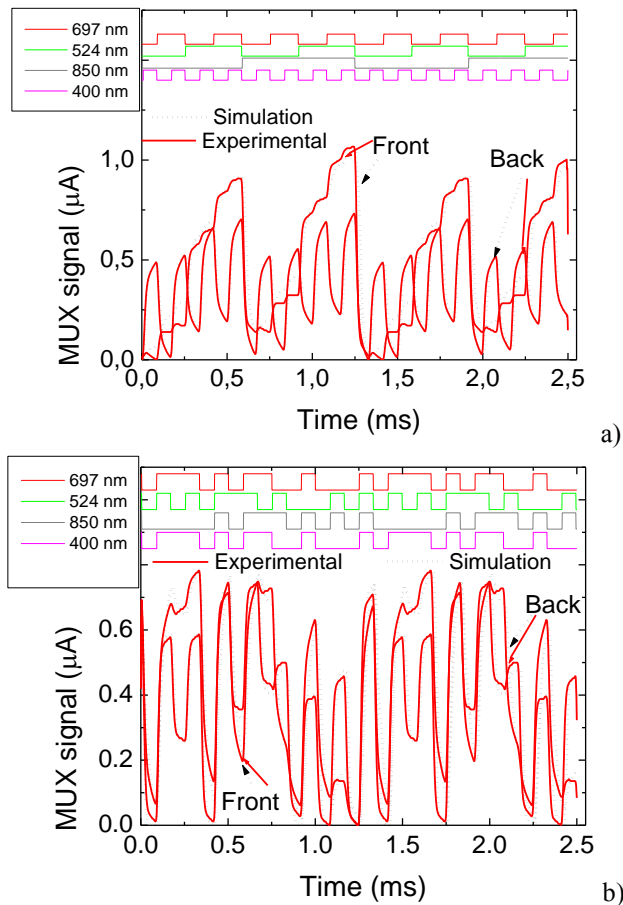


Figure 8. Numerical simulation with front and back  $\lambda=390$  nm irradiation, and different channel wavelength combinations and bit sequences.

A good fitting between experimental and simulated results was achieved. The plots show the ability of the presented model to simulate the sensitivity behavior of the proposed system in the visible/infrared spectral ranges. The optoelectronic model with light biasing control has proven to be a good tool to design optical filters. Furthermore, this model allows for extracting theoretical parameters by fitting the model to the measured data (internal resistors and capacitors). Under back irradiation higher values of  $C_2$  were obtained confirming the capacitive effect of the near-UV radiation on the device that increases the charge stored in the space charge layers of the back optical gate of  $Q_2$  modelled by  $C_2$ .

## VI. CONCLUSIONS

We experimentally and theoretically demonstrate the use of near-ultraviolet steady state illumination to increase the spectral sensitivity of a double a-SiC/Si pi-n/pin photodiode beyond the visible spectrum (400 nm-880 nm). The concept is extended to implement a 1 by 4 wavelength division multiplexer with channel separation in the visible/near infrared ranges.

Results show that, the pi-n/pin multilayered structure becomes reconfigurable under front and back irradiation, acting as data selector in the VIS/NIR ranges. The device performs WDM optoelectronic logic functions providing photonic functions such as signal amplification, filtering and switching. The opto-electrical model with light biasing control has proven to be a good tool to design optical filters in the VIS/NIR. An optoelectronic model was presented and proven to be a good tool to design optical filters in the VIS/NIR range.

## ACKNOWLEDGEMENTS

This work was supported by FCT (CTS multi annual funding) through the PIDDAC Program funds (UID/EEA/00066/2013) and PTDC/EEA-ELC/120539/2010.

## REFERENCES

- [1] T. Komiyama, K. Kobayashi, K. Watanabe, T. Ohkubo, and Y. Kurihara, "Study of visible light communication system using RGB LED lights," in Proceedings of SICE Annual Conference, IEEE, 2011, pp. 1926–1928.
- [2] S. S. Djordjevic et al. "Fully Reconfigurable Silicon Photonic Lattice Filters With Four Cascaded Unit Cells" IEEE photonics Technology Letters, 23, NO. 1, january 1, 2011, pp. 41-44.
- [3] P. P. Yupapin and P. Chunpang, "An Experimental Investigation of the Optical Switching Characteristics Using Optical Sagnac Interferometer Incorporating One and Two Resonators," Optics & Laser Technology, Vol. 40, No. 2, 2008, pp. 273-277.
- [4] S. Ibrahim et al., "Fully Reconfigurable Silicon Photonic Lattice Filters With Four Cascaded Unit Cells" 21 Mar 2010, paper OWJ5. Optical Fibre Communications Conference, OSA/OFC/NFOEC, San Diego.
- [5] M. Vieira, P. Louro, M. Fernandes, M. A. Vieira, A. Fantoni, and J. Costa, "Three Transducers Embedded into One Single SiC Photodetector: LSP Direct Image Sensor, Optical Amplifier and Demux Device", Advances in Photodiodes", InTech, Chap.19, 2011, pp. 403-425.
- [6] M. Vieira, P. Louro, M. Fernandes, M. A. Vieira, A. Fantoni, and J. Costa Advances in Photodiodes, InTech, Chap.19, 2011, pp:403-425.
- [7] M.A. Vieira, P. Louro, M. Vieira, A. Fantoni, and A. Steiger-Garção, "Light-activated amplification in Si-C tandem devices: A capacitive active filter model" IEEE sensor jornal, 12, NO. 6, 2012, pp. 1755-1762.
- [8] M. A. Vieira, M. Vieira, P. Louro, V. Silva, and A. S. Garção, "Photodetector with integrated optical thin film filters" Journal of Physics: Conference Series, 421, 012011 March 2013. doi:10.1088/1742-6596/421/1/012011
- [9] M. Vieira, M. A. Vieira, I. Rodrigues, V. Silva, and P. Louro, "Tuning optical a-SiC/a-Si active filters by UV bias light in the visible and infrared spectral ranges", Phys. Status Solidi, C, 2014, pp. 1-4 Article first published online: 25 JUL 2014. DOI: 10.1002/pssc.201400020.